FlowVLA: Visual Chain of Thought-based Motion Reasoning for Vision-Language-Action Models

Zhide Zhong[1], **Haodong Yan**[1], **Junfeng Li**[1], **Xiangchen Liu**[1], **Xin Gong**[1], **Tianran Zhang**[1], **Wenxuan Song**[1], **Jiayi Chen**[1], **Xinhu Zheng**[1], **Hesheng Wang**[2], **and Haoang Li** [1]

[1]HKUST(GZ), [2]Shanghai Jiao Tong University

Many Vision-Language-Action (VLA) models are built upon an internal world model trained via next-frame prediction "$v_t \rightarrow v_{t+1}$". However, this paradigm attempts to predict the future frame's appearance directly, without explicitly reasoning about the underlying dynamics. This lack of an explicit motion reasoning step often leads to physically implausible visual forecasts and inefficient policy learning. To address this limitation, we introduce the **Visual Chain of Thought**, a paradigm that compels the model to first reason about motion dynamics before generating the future frame. We instantiate this paradigm by proposing **FlowVLA**, an autoregressive Transformer that explicitly materializes this reasoning process as "$v_t \rightarrow f_t \rightarrow v_{t+1}$", where f_t is an intermediate optical flow prediction that inherently encodes motion. By forcing the model to first follow the motion plan encoded by f_t, this process aligns the pre-training objective of dynamics prediction with the downstream task of action generation. We conduct experiments on challenging robot manipulation benchmarks, as well as a real-robot platform. Our FlowVLA not only generates more coherent and physically plausible visual predictions, but also achieves state-of-the-art policy performance with substantially improved sample efficiency, pointing toward a more principled foundation for world modeling in VLAs. Project page: https://irpn-lab.github.io/FlowVLA/

Keywords: Visual Chain of Thought, World Models, Vision-Language-Action Models

1. Introduction

Robotics manipulation in diverse and unstructured environments Kim et al. (2024a), Zhou et al. (2025), Xu et al. (2025) has been a long-standing challenge, requiring both precise action prediction and robust understanding of visual and linguistic cues. Recent advances in Vision-Language-Action (VLA) models Kim et al. (2024b), Zitkovich et al. (2023), Black et al. (2024), Team et al. (2024), particularly those pre-trained as world models like UniVLA Wang et al. (2025) and WorldVLA Cen et al. (2025), have shown remarkable promise for creating generalist robots capable of tackling such manipulation tasks. The prevailing strategy involves training a large autoregressive transformer to predict the next visual frame given past observations, effectively learning the dynamics of the environment from vast amounts of video data. This learned world model then serves as a powerful foundation for fine-tuning downstream action policies.

Despite their success, these models suffer from a critical and foundational flaw: they attempt to predict the next frame[1] in a single, direct step, without explicitly considering the underlying physical motion. This next-frame prediction paradigm is often a "pixel-copying trap" Ming et al. (2024), where the model learns to replicate static backgrounds without a deep understanding of spatiotemporal dynamics, leading to blurry, inconsistent, and physically implausible long-horizon forecasts. Furthermore, this approach creates

[1] Throughout this paper, "frame" denotes a sampled key frame from the video sequence rather than an immediately adjacent frame.

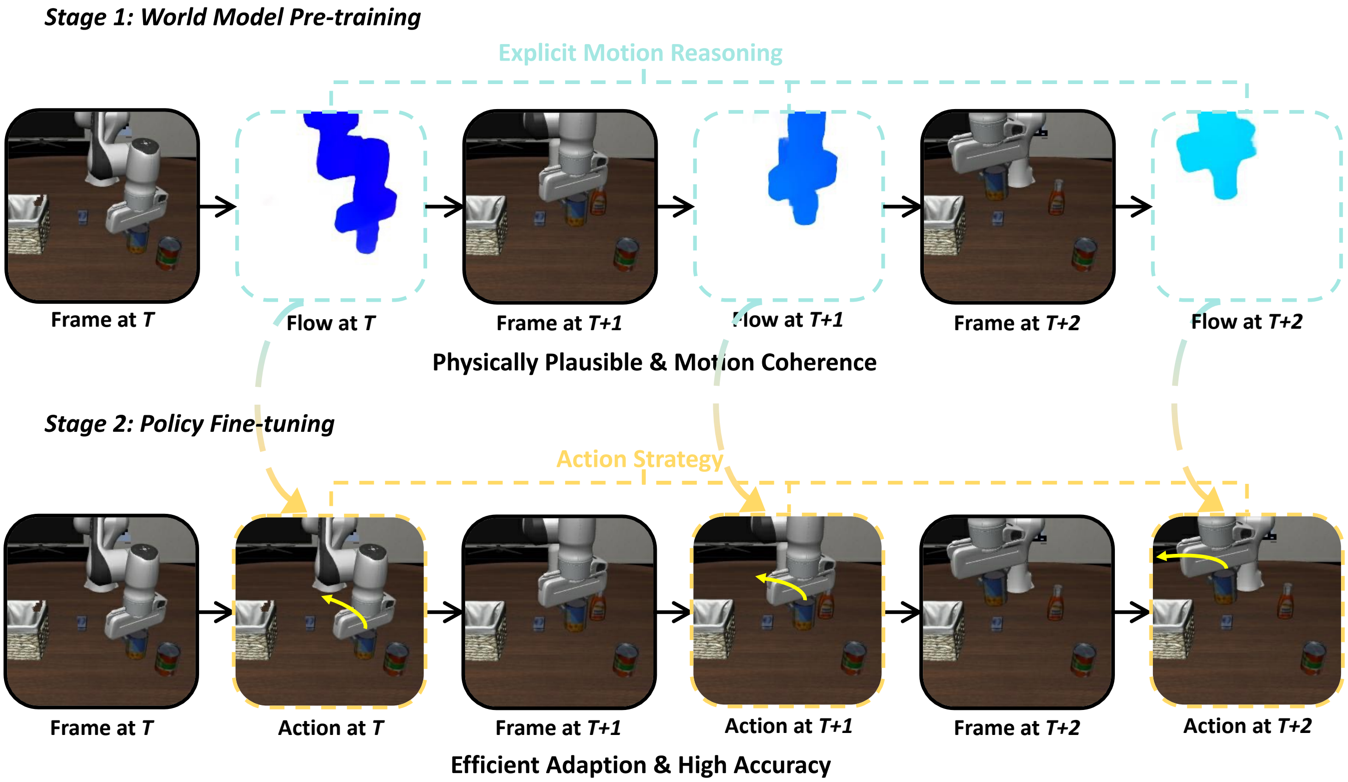
Stage 1: World Model Pre-training
Explicit Motion Reasoning
Frame at T
Flow at T
Frame at T+1
Flow at T+1
Frame at T+2
Flow at T+2
Physically Plausible & Motion Coherence
Stage 2: Policy Fine-tuning
Action Strategy
Frame at T
Action at T
Frame at T+1
Action at T+1
Frame at T+2
Action at T+2
Efficient Adaption & High Accuracy

Figure 1: Two-Stage Training Paradigm of FlowVLA. (Top) Stage 1: World Model Pre-training with Visual CoT. The model learns to predict an intermediate motion representation (Flow at T) from an initial frame (Frame at T), and then forecasts the subsequent frame (Frame at $T+1$). This iterative process yields physically plausible, long-horizon video predictions. **(Bottom) Stage 2: Policy Fine-tuning.** Through fine-tuning, the pre-trained world model is adapted to generate precise robot action chunk (Action at T) from visual observations. This paradigm leverages the learned dynamics for efficient and accurate policy learning.

a significant domain gap between the passive, observational knowledge learned during pre-training and the active, action-oriented knowledge required for policy learning. This results in inefficient knowledge transfer and requires extensive fine-tuning, as evidenced by slow convergence on downstream tasks Zeng et al. (2024).

One of the main reasons for the unsatisfactory performance of the above methods is that they attempt to learn a direct, unreasoned mapping from the current frame to the next, thereby bypassing the crucial step of physical reasoning. Drawing inspiration from the success of Chain of Thought prompting in Large Language Models Wei et al. (2022), which enhances reasoning by generating intermediate steps, we propose a novel paradigm for world models: a **Visual Chain of Thought (Visual CoT)**. Instead of a single, opaque leap from the current frame v_t to the next v_{t+1}, we decompose the prediction into a structured reasoning process. First, predict the intermediate physical dynamics—the optical flow f_t that describes *how* every pixel will move. Then, conditioned on this explicit motion plan, predict the resulting future frame. This $v_t \to f_t \to v_{t+1}$ causal chain (see Figure 1, top) transforms the learning objective from mere pattern recognition into a structured physical reasoning task. By explicitly modeling dynamics, the world model learns representations that are inherently more aligned with the action-centric knowledge required for policy learning.

To fully leverage the above physically grounded world model for robot action prediction, we propose **FlowVLA**, a model that realizes the abstract dynamics step using optical flow as the concrete motion representation.

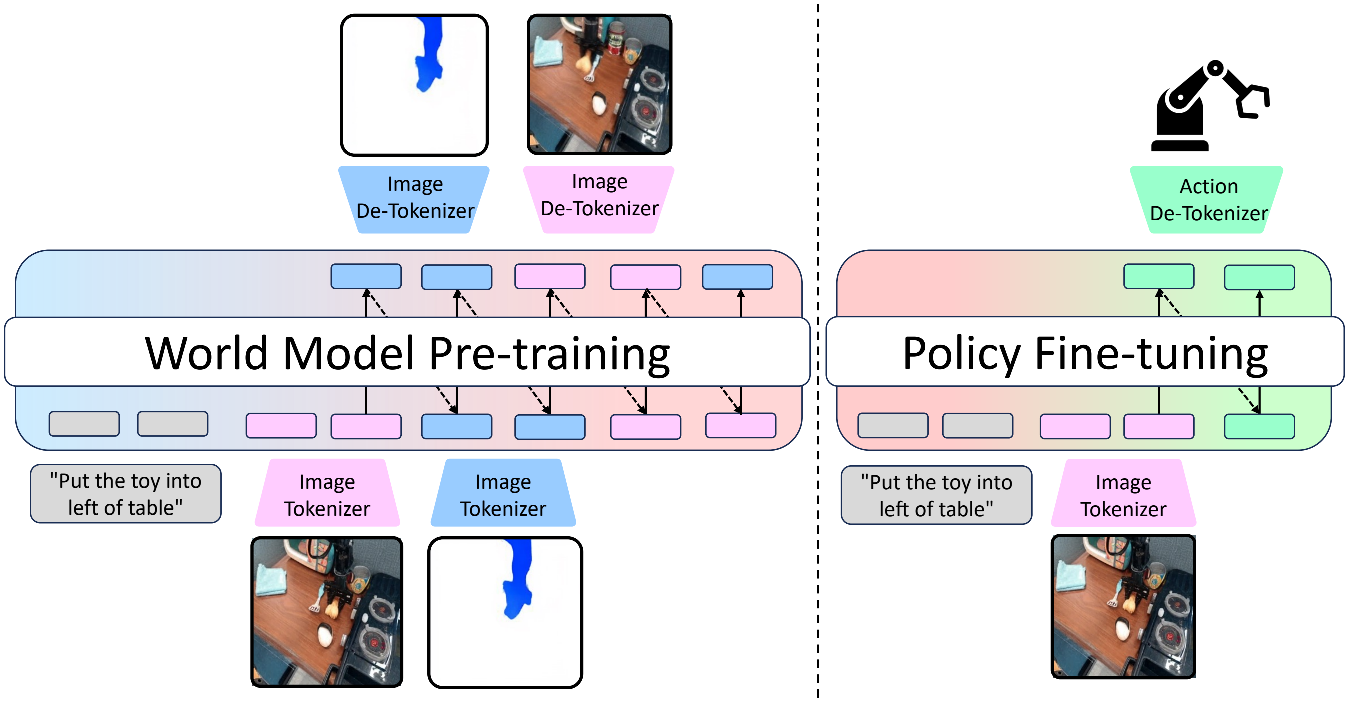

Figure 2: Model Architecture of FlowVLA. Our model instantiates the two-stage training paradigm in Figure 1. **(Left) Stage 1: World Model Pre-training with Visual CoT.** Input frames are encoded into appearance tokens (pink). The model then autoregressively predicts an interleaved sequence of motion tokens (blue) and future appearance tokens. Our proposed $v_t \rightarrow f_t \rightarrow v_{t+1}$ prediction forces the model to reason about dynamics before forecasting the future. For conceptual clarity, the Image and Flow Tokenizers are visualized separately; in practice, they are the exact same module applied to both appearance and motion inputs. **(Right) Stage 2: Policy Fine-tuning.** The pre-trained world model is adapted for action prediction. Conditioned on a text instruction (gray) and the current observation (magenta), the model autoregressively predicts action tokens (green) that are decoded into robot action chunk.

Our training paradigm proceeds in **two stages** as illustrated in Figure 1. *Stage 1: World Model Pre-training with Visual CoT* focuses on visual reasoning, where the model is pre-trained on large-scale videos to master physically plausible and motion-coherent future frame forecasting. *Stage 2: Policy Fine-tuning* adapts this pre-trained world model for action prediction: given a text instruction and current observation, the model now predicts discrete robot action chunk instead of future frames. Because Stage 1 has already aligned visual and dynamics representations with physical reality, Stage 2 can fine-tune the policy with substantially improved sample efficiency, directly benefiting from the explicit motion reasoning learned during World Model Pre-training with Visual CoT.

A key aspect of our design is to integrate motion without introducing dedicated architectural components. We encode optical flow fields by a flow map, allowing them to be processed by the exact same Vector Quantization (VQ) tokenizer as regular camera observations. This enables a single, unmodified autoregressive transformer to seamlessly learn the interleaved sequence of appearance and motion tokens. This design makes FlowVLA a truly Unified Visual CoT, where the reasoning steps (flows) and states (frames) are expressed in a shared vocabulary and processed by a single, unified model.

Our work makes the following contributions:

- We identify a fundamental limitation of next-frame prediction and propose Visual Chain of Thought

(Visual CoT) as a new paradigm for learning dynamics for VLA world models, explicitly modeling motion to better bridge the gap between world model pre-training and policy fine-tuning.
- We introduce FlowVLA, an effective instantiation of this paradigm that unifies appearance and motion reasoning within a single autoregressive Transformer via shared tokenization, avoiding task-specific architectural components and enabling seamless integration of motion reasoning into world model pre-training.
- We demonstrate through extensive experiments that FlowVLA achieves state-of-the-art performance on challenging manipulation benchmarks and a real-robot platform, while offering superior sample efficiency.

2. Methodology

In this section, we introduce FlowVLA, a novel framework designed to instantiate our proposed Visual Chain of Thought (Visual CoT) paradigm. Firstly, we present our Visual CoT formulation. Secondly, We provide a high-level overview of our two-stage training. Thirdly, we detail the Visual CoT pre-training stage, including our unified tokenization scheme for appearance and motion. Finally, we describe how the learned world model is finetuned for downstream robotics tasks.

2.1. Visual Chain of Thought

The paradigm for pre-training world models is next-frame prediction. This approach aims to learn a probabilistic model, typically parameterized by a large Transformer parameterized by θ, that predicts the next visual observation v_{t+1} given a history of past observations and a guiding language instruction L. The learning objective can be expressed as maximizing the log-likelihood of the next frame:

$$\max_{\theta} \mathbb{E}_{(v_t, v_{t+1}, L)\sim\mathcal{D}}[\log P_{\theta}(v_{t+1}|v_t, L)]. \tag{1}$$

While conceptually simple and scalable to large and unlabeled video datasets $\mathcal{D}$, this formulation suffers from fundamental limitations that hinder the acquisition of robust physical reasoning.

To overcome the aforementioned challenges, we reframe the world modeling task by introducing a **Visual Chain of Thought (Visual CoT)**. Inspired by the success of CoT in large language models Wei et al. (2022), which improves reasoning by generating intermediate steps, we propose to decompose the visual prediction process. Instead of a single, unreasoned leap, we compel the model to first "think" about the intermediate physical process before generating the final outcome. We instantiate this "thought" as the dense optical flow field f_t, which describes the per-pixel motion from v_t to v_{t+1}.

Formally, we reformulate the task from modeling $P(v_{t+1}|v_t, L)$ in Equation (1) to modeling the joint probability $P(v_{t+1}, f_t|v_t, L)$. By applying the chain rule of probability, we factorize this joint probability into a causal sequence:

$$P(v_{t+1}, f_t|v_t, L) = \underbrace{P(v_{t+1}|f_t, v_t, L)}_{\text{Appearance Generation}} \times \underbrace{P(f_t|v_t, L)}_{\text{Motion Reasoning}} . \tag{2}$$

This decomposition offers several key advantages. It decouples the learning problem, allowing the model to first focus on the physically-grounded *Motion Reasoning* task before tackling the more appearance-focused *Appearance Generation* task. It introduces a powerful **inductive bias**, explicitly guiding the model to learn a representation of motion, thereby grounding its predictions in physical causality. Crucially, this **aligns** the pre-training objective with the needs of downstream action prediction. A model that explicitly understands motion f_t is inherently better prepared to generate an action chunk a_t that cause desired motions.

The above reformulation addresses the limitations of the direct next-frame prediction paradigm. From a learning perspective, the objective function in Equation (1) is fundamentally ill-posed. It frames world modeling as a high-dimensional regression problem directly in pixel space, which creates an optimization landscape fraught with trivial local minima. This often manifests as the "pixel-copying trap" Ming et al. (2024), where the model discovers that the easiest way to minimize reconstruction error is to simply replicate static background pixels from the input frame. This optimization shortcut is a primary cause of the blurry, inconsistent, and physically implausible forecasts observed in models trained with this paradigm. Furthermore, this direct mapping $v_t \rightarrow v_{t+1}$ lacks an explicit **causal structure**. The model learns a direct correlation between pixel configurations over time, which may not correspond to the true physical causal relationships. This reliance on correlation over causation results in sensitive models that fail to generalize to out-of-distribution scenarios where visual cues change, even if the underlying physics remain the same.

2.2. Framework Overview

As shown in Figure 2, FlowVLA follows a two-stage training paradigm, consistent with state-of-the-art methods like UniVLA Wang et al. (2025) and WorldVLA Cen et al. (2025) to ensure a fair basis for comparison.

1. Stage 1: World Model Pre-training: The model learns general physical dynamics from large-scale, action-free video data by executing our proposed Visual Chain of Thought.
2. Stage 2: Policy Finetuning: The pre-trained model weights are finetuned on downstream, action-annotated robotics datasets to learn specific control policies.

2.3. Stage 1: World Model Pre-training via Visual Chain of Thought

The goal of this stage is to learn a robust world model by compelling it to reason about dynamics before predicting future states. This is achieved through our Visual Chain of Thought (Visual CoT) pre-training task. Below, we detail the tokenization scheme that unifies appearance and motion, and then describe the autoregressive objective used to learn the reasoning chain.

Unified Motion and Appearance Tokenization A cornerstone of FlowVLA's design is a unified tokenization scheme that represents two physically distinct signals—appearance (images) and motion (optical flow)—within a single, shared vocabulary. This approach preserves architectural simplicity and promotes the learning of deep cross-modal representations. To achieve this, we process each modality as follows.

For the **Appearance Representation**, standard RGB frames v_t, which capture the static appearance of the scene, are processed by a pretrained VQ-GAN tokenizer Esser et al. (2021). This tokenizer discretizes each high-resolution image into a compact grid of visual tokens from a learned codebook. This tokenized representation allows the Transformer to process complex visual information in the same sequential format as text.

For the **Motion Representation**, we encode the abstract motion dynamics using optical flow f_t. It is a dense pixel-level representation that describes the projected motion of every point in the visual field between two consecutive frames. We choose optical flow for its ability to capture fine-grained interaction dynamics, such as sliding, pushing, and rotating. Another advantage is the availability of robust off-the-shelf models, such as RAFT Teed and Deng (2020), for pre-computation from video data.

We choice optical flow instead of object-centric alternatives like 3D poses or bounding boxes for two main reasons. First, acquiring such object-level representations accurately often requires specialized upstream models trained on large, manually annotated datasets, limiting scalability and introducing potential points of failure. Second, these sparse representations cannot capture non-rigid motion or complex interaction dynamics. In contrast, optical flow provides a dense, general signal that is independent of object detectors. Therefore, it naturally represents continuous motion.

Critically, the image structure of optical flow allows for a shared tokenizer with RGB frames, ensuring tight modality alignment and architectural simplicity. These "flow maps" are then processed by the exact same VQ-GAN tokenizer used for the RGB frames. This design is central to our framework's efficiency and simplicity, yielding three significant benefits. First, it provides **Parameter Efficiency**, as no new motion-specific tokenizer or architectural modules are required. Second, it maintains **Architectural Simplicity** through a single, end-to-end autoregressive pipeline without specialized branches. Finally, it fosters a **Unified Representation**, encouraging the model to learn deep correlations between appearance ("what is there") and motion ("how it moves") within a shared latent space.

To integrate optical flow into our unified framework, we convert the 2-channel flow fields (containing displacements u and v) into standard 3-channel RGB images. This conversion, following the technique from VideoJAM Chefer et al. (2025), maps the motion vector at each pixel to a color based on its polar coordinates. Unlike traditional optical flow visualizations that often normalize motion magnitude by the global maximum displacement in a frame, causing subtle motions to be visually suppressed, VideoJAM applies a fixed scaling coefficient and non-linear normalization strategy, which preserves fine-grained motion cues while avoiding saturation in high-speed regions. The direction of motion is mapped to the color's Hue (from angle $\alpha = \arctan 2(v, u)$), and the speed of motion is mapped to the color's Saturation and Value (from magnitude $m = \sqrt{u^2 + v^2}$). To handle a wide range of motion speeds without saturation or loss of detail for subtle movements, the magnitude is non-linearly normalized to the range $[0, 1]$ using a scaling coefficient $\sigma = 0.15$:

$$m_{\text{norm}} = \min\left(1.0, \frac{m}{\sigma \cdot \sqrt{H^2 + W^2}}\right), \tag{3}$$

where H and W are the frame's height and width.

Autoregressive Learning of the Visual CoT With a unified token representation for both frames (v_t) and flow (f_t), we construct a reasoning chain $v_t \rightarrow f_t \rightarrow v_{t+1}$. We employ a standard decoder-only Transformer, training it to predict an interleaved sequence of frames and optical flow fields given an optional language instruction L_{instr}:

$$S_{\text{wm}} = \{L_{\text{instr}}, v_0, f_0, v_1, f_1, \ldots, v_T, f_T\} \tag{4}$$

The model is trained using a standard next-token prediction objective, maximizing the log-likelihood of the sequence. The loss of the world model, $\mathcal{L}_{\text{WM}}$, is the sum of the cross-entropy losses in both the reasoning step (flow tokens) and the final state (next frame tokens). Formally, for each timestep t, the model first predicts the flow f_t based on all preceding tokens, and then predicts the next frame v_{t+1} conditioned on both the history and the just-predicted flow:

$$\mathcal{L}_{\text{WM}} = \sum_{t=0}^{T-1} \left(\mathcal{L}_{\text{CE}}(f_t | S_{<v_{t+1}}) + \lambda \cdot \mathcal{L}_{\text{CE}}(v_{t+1} | S_{<v_{t+1}}, f_t)\right) \tag{5}$$

where $S_{<v_{t+1}}$ denotes all the tokens preceding v_{t+1}, and λ is a balancing hyperparameter (set to 1.0 in our experiments). This objective explicitly forces the model to perform a "reason → predict" process during both training and inference.

2.4. Stage 2: Finetuning for Action Prediction

Initialization and Task. The policy model is initialized with the weights from the pre-trained world model. During this stage, the input sequence is composed of interleaved observations and actions: $S_{\text{policy}} = \{L_{\text{instr}}, v_0, a_0, v_1, a_1, \ldots\}$, where a_t represents the robot's action tokens.

Action Tokenization and Objective. Actions are discretized into tokens following the FAST Pertsch et al. (2025). Critically, the fine-tuning loss, $\mathcal{L}_{\text{policy}}$, is computed only over the action tokens. This objective directs the model to leverage all its learned visual and dynamical knowledge towards the singular goal of making correct action prediction.

3. Experiments

We conduct a comprehensive set of experiments to validate the effectiveness of our proposed Visual Chain of Thought framework. Our evaluation is designed to answer four key questions:

Q1: Does FlowVLA achieve state-of-the-art performance on complex, long-horizon robotics tasks?
Q2: Does explicit motion reasoning lead to superior world modeling capabilities compared with approaches that learn world dynamics implicitly?
Q3: Is FlowVLA more sample-efficient during policy fine-tuning, validating our claim of bridging the pre-training/fine-tuning gap?
Q4: What is the effectiveness of each key component in our model architecture?

3.1. Experimental Setup

To comprehensively assess FlowVLA's capabilities, we conduct evaluations across a suite of complementary settings. We use two challenging simulation benchmarks, LIBERO and SimplerEnv, to measure generalization and robustness against domain shifts. Additionally, we perform Real-Robot experiments to validate the model's practical applicability and its ability to transfer skills from simulation to reality.

LIBERO Benchmark. We evaluate FlowVLA on the LIBERO benchmark Liu et al. (2023) to assess its generalization across multiple axes. Following the standard behavioral cloning setup, we report performance on its four main suites, which test for generalization to novel spatial layouts, objects, task goals, and long-horizon compositional challenges.

SimplerEnv Benchmark. We use SimplerEnv Li et al. (2024) to assess the model's robustness against significant domain shifts. This benchmark is specifically designed to evaluate policy transfer by introducing diverse variations in lighting, textures, and camera viewpoints, which are more representative of real-world complexity.

Real-world Experiments based on AgileX Cobot. As shown in Figure 3(a), we conduct our real-world experiments on a Cobot dual-arm robot manufactured by AgileX Robotics, which adopts the Mobile ALOHA system design Fu et al. (2024). Each arm has 7 degrees of freedom and is equipped with a parallel gripper.

The robot carries multiple onboard sensors, including wrist-mounted cameras on both arms and a front-facing camera, for capturing RGB observations used as model input. We design four manipulation tasks to comprehensively evaluate the model's spatial reasoning and control capabilities (see Figure 3(b)). For each task, we collect 50–200 human-teleoperated demonstrations for fine-tuning, thereby evaluating the model's data efficiency and its ability to rapidly adapt to the specific embodiment of the Cobot platform.

Implementation Details. Our FlowVLA model is built on the 8.5B parameter Emu3 Wang et al. (2024) and UniVLA Wang et al. (2025) architecture. We incorporate optical flow, pre-computed with RAFT Teed and Deng (2020), as an additional modality to represent motion. We follow the standard training setup for the LIBERO and SimplerEnv benchmarks Kim et al. (2024b, 2025). For LIBERO, we pre-train the world model for 5k steps with a batch size of 16, and then fine-tune the policy for 5k steps with a batch size of 96. For the SimplerEnv benchmark, pre-training runs for 12k steps with a batch size of 32 and policy fine-tuning for 20k steps with a batch size of 128.

3.2. Evaluations Results (Q1)

To answer Q1, we evaluate the final performance of FlowVLA after policy finetuning on both benchmarks. Our method establishes a new state-of-the-art on both, demonstrating its effectiveness and robustness.

Results on LIBERO. As shown in Table 1, FlowVLA consistently outperforms all prior methods across the four evaluated suites. Notably, the performance gains are most significant on the *Long* horizon tasks. This directly highlights the benefit of learning a world model with a more robust understanding of physical dynamics, as our Visual CoT framework enables better long-term planning and reasoning.

Results on SimplerEnv. We further test our model's robustness on the SimplerEnv benchmark, which introduces significant visual domain shifts. Table 2 shows that FlowVLA achieves a substantial improvement over existing methods. The remarkable success on tasks that were previously challenging for other models (e.g., stacking blocks) validates that our explicit motion reasoning leads to policies that are more resilient to the visual and physical variations found in more realistic environments.

Results on Real-Robot. As shown in Table 3, FlowVLA exhibits clear advantages over all baselines across the four real-world Cobot tasks, including both single-arm and bimanual operations. The improvements are particularly pronounced in more complex bimanual tasks such as *Placing two cola cans into a box* and *Lifting a pot using both arms*, where precise coordination and dynamic interaction are required. During evaluation, each task was executed 25 times to ensure statistically reliable success rates. These results confirm that FlowVLA's explicit motion reasoning and world model-based long-horizon planning are effective in real-world settings, enabling rapid adaptation to the specific embodiment and visual conditions of the Cobot platform.

3.3. Analysis of World Modeling Capabilities (Q2)

To demonstrate the superiority of our motion reasoning framework compared with approaches that learn world dynamics implicitly, we conduct a detailed qualitative analysis on the challenging, real-world Bridge V2 dataset. The standard next-frame prediction baseline suffers from two distinct and critical failure modes.

- **Failures in Physical Plausibility.** As highlighted in Figure 4, the baseline model generates physically incoherent rollouts, such as causing the robotic arm to suddenly vanish or producing inconsistent object motion. This indicates a fundamental inability to model the basic physical continuity of a scene.

Table 1: Results on the LIBERO Benchmark Liu et al. (2023). We report the final task success rate (%) and compare FlowVLA against state-of-the-art methods, grouped by their core methodology. The results demonstrate that our Visual CoT pre-training leads to superior performance, highlighting the efficiency of our proposed framework.

Model	Large Scale Pretrain	Spatial	Object	Goal	Long	**Avg.**
w/o World Model						
Diffusion Policy Chi et al. (2023)	×	78.3	92.5	68.3	50.5	72.4
Octo Team et al. (2024)	✓	78.9	85.7	84.6	51.1	75.1
OpenVLA Kim et al. (2024b)	✓	84.7	88.4	79.2	53.7	76.5
DiT Policy Hou et al. (2025)	✓	84.2	96.3	85.4	63.8	82.4
TraceVLA Zheng et al. (2024)	✓	84.6	85.2	75.1	54.1	74.8
SpatialVLA Qu et al. (2025)	✓	88.2	89.9	78.6	55.5	78.1
pi0-FAST Pertsch et al. (2025)	✓	96.4	96.8	88.6	60.2	85.5
ThinkAct Huang et al. (2025a)	✓	88.3	91.4	87.1	70.9	84.4
w/ World Model						
WorldVLA Cen et al. (2025)	×	85.6	89.0	82.6	59.0	79.1
UniVLA† Wang et al. (2025)	×	92.6	93.8	86.6	63.0	84.0
CoT-VLA Zhao et al. (2025)	✓	87.5	91.6	87.6	69.0	81.1
FlowVLA (ours)	×	**93.2**	**95.0**	**91.6**	**72.6**	**88.1**

† Our reported UniVLA result is from our re-implementation, pre-trained only on LIBERO without wrist camera images for a fair comparison.

Table 2: Results on the SimplerEnv-WidowX benchmark Li et al. (2024). We report the final task success rate (%). FlowVLA significantly surpasses prior methods, demonstrating superior robustness to the visual domain shifts present in this benchmark. Best results are in **bold**.

Model	Put Spoon	Put Carrot	Stack Block	Put Eggplant	**Avg.**
RT-1-X Team et al. (2024)	0.0	4.2	0.0	0.0	1.1
Octo-Base Team et al. (2024)	12.5	8.3	0.0	43.1	16.0
Octo-Small Team et al. (2024)	47.2	9.7	4.2	56.9	29.5
OpenVLA Team et al. (2024)	0.0	0.0	0.0	4.1	1.0
RoboVLMs Liu et al. (2025)	45.8	20.8	4.2	79.2	37.5
SpatialVLA Qu et al. (2025)	16.7	25.0	29.2	100	42.7
RoboPoint Yuan et al. (2024)	16.7	20.8	8.3	25.0	17.7
FSD Yuan et al. (2025a)	41.6	50.0	33.3	37.5	40.6
Embodied-R1 Yuan et al. (2025b)	62.5	**68.0**	36.1	58.3	56.2
ThinkAct Huang et al. (2025a)	58.3	37.5	8.7	70.8	43.8
UniVLA† Wang et al. (2025)	62.5	62.5	41.6	95.8	65.6
FlowVLA (Ours)	**70.8**	62.5	**62.5**	**100.0**	**74.0**

† Result obtained by evaluating the officially released checkpoint.

- **Semantic Inconsistency.** Figure 5 illustrates a more subtle but equally critical issue. While the predicted frames from the baseline may appear visually coherent, the depicted action fails to follow the

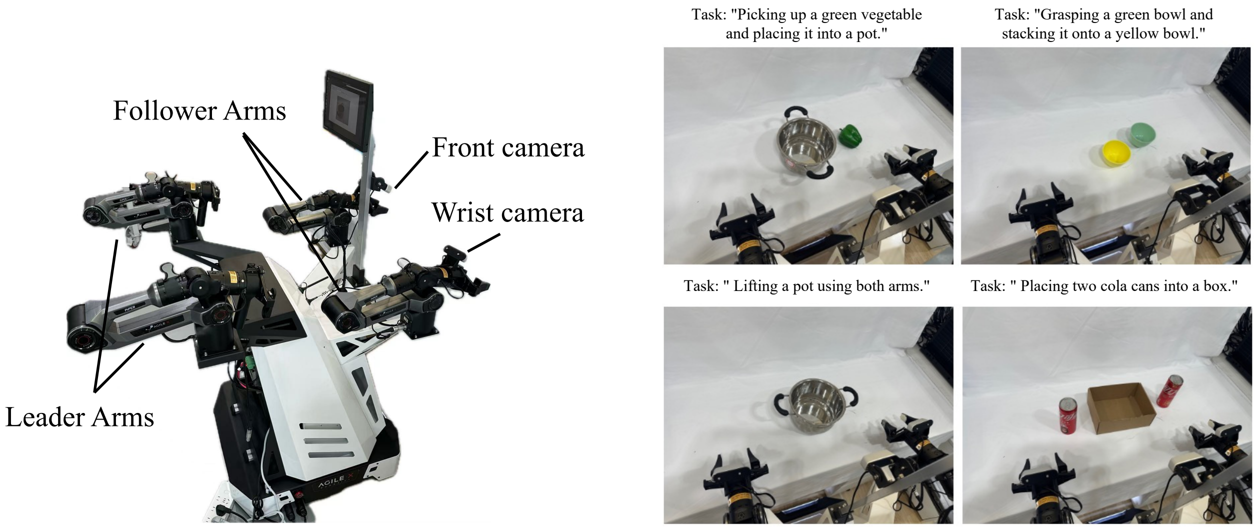
Follower Arms
Front camera
Wrist camera
Leader Arms
Task: "Picking up a green vegetable and placing it into a pot."
Task: "Grasping a green bowl and stacking it onto a yellow bowl."
Task: " Lifting a pot using both arms."
Task: " Placing two cola cans into a box."

(a) Platform setup

(b) Example tasks

Figure 3: AgileX Cobot dual-arm platform and real-world manipulation tasks: (a) system setup: leader arms are user-operated, follower arms mirror the actions. Vision is provided by a front camera for global scene view and wrist cameras for close-up workspace observation. (b) representative single-arm and bimanual operations: from simple single-arm tasks to complex long-horizon bimanual manipulations.

Table 3: Results on the Real-world AgileX Cobot platform. We report the task success rates (%). The evaluation covers four manipulation tasks of varying difficulty, from single-arm to bimanual operation. Best results are in **bold**.

Model	Stack Bowls	Place Vegetable	Place Bottles	Lift Pot	**Avg.**
ACT Zhao et al. (2023)	32.0	24.0	12.0	8.0	19.0
OpenVLA Kim et al. (2024b)	28.0	20.0	20.0	12.0	20.0
UniVLA Wang et al. (2025)	48.0	40.0	16.0	20.0	31.0
FlowVLA (Ours)	**56.0**	60.0	**32.0**	**28.0**	**44.0**

given language command. This reveals a disconnection between language understanding and visual forecasting.

In contrast, FlowVLA successfully overcomes the above challenges. By first reasoning about motion dynamics via optical flow, our model generates predictions that are not only physically plausible but also semantically aligned with the task instructions, showcasing the robustness and generalizability of our approach.

3.4. Convergence Speed and Data Efficiency(Q3)

To isolate and evaluate the impact of our Visual CoT pre-training, we conduct a direct comparison between FlowVLA and its foundational baseline, UniVLA. Figure 6 illustrates FlowVLA's dramatic advantage in training and sample efficiency. In the full-data setting (Figure 6(a)), FlowVLA proves vastly more sample-efficient, reaching the baseline's peak performance (0.64) with only **one-third of the training steps** (2k vs. 6k) while also achieving a higher final success rate of 0.73.

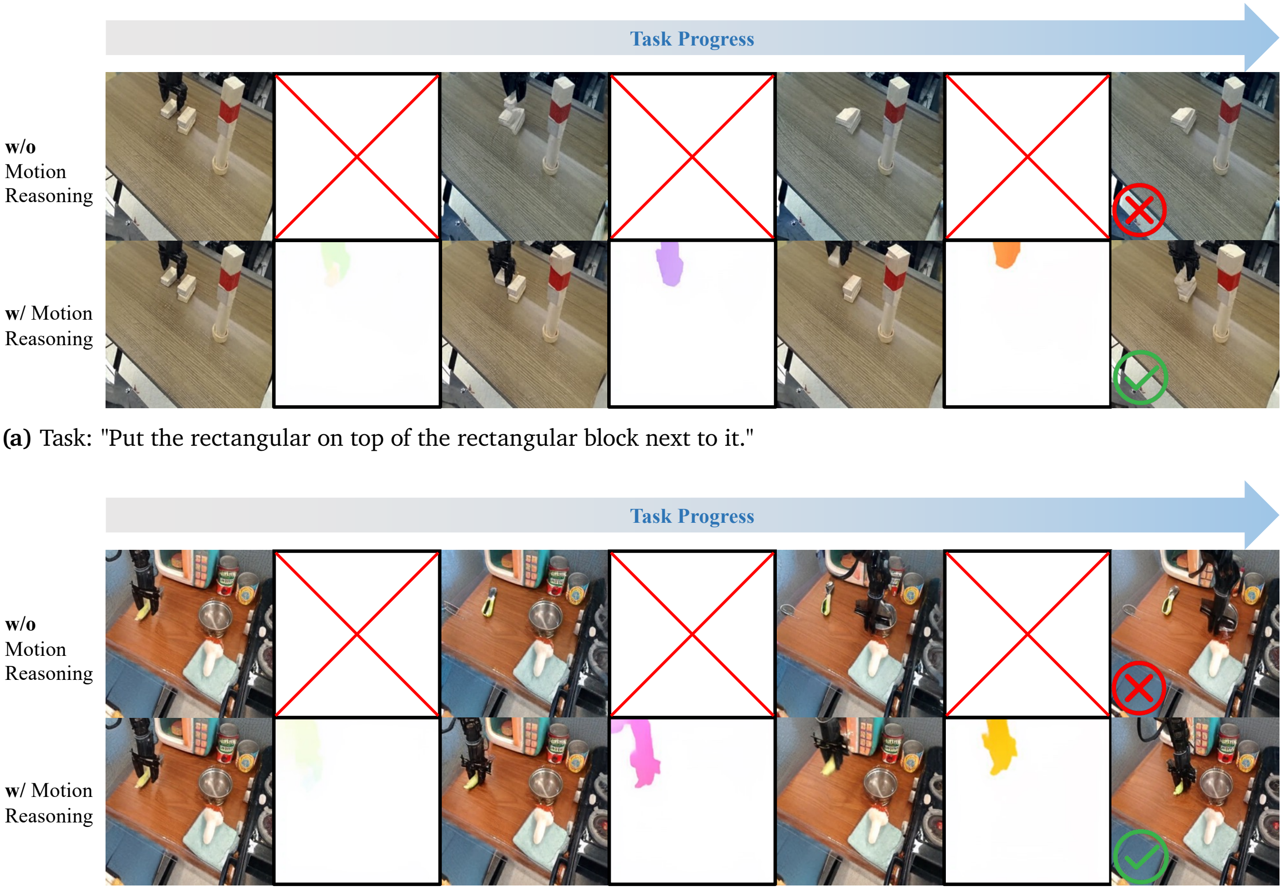

(a) Task: "Put the rectangular on top of the rectangular block next to it."

(b) Task: "Move the spoon so that it sits to the left of the metal pot."

Figure 4: Analysis of Physical Plausibility on the Bridge V2 Dataset. This figure highlights common physical failures in the baseline model. In both examples, the baseline model (top row) struggles to maintain physical consistency, leading to implausible outcomes such as a disappearing manipulator or erratic object behavior. In contrast, **FlowVLA** (bottom row), guided by its motion-first reasoning, produces stable and physically coherent predictions that accurately reflect the scene's dynamics.

This efficiency advantage is amplified in the more challenging low-data regime (Figure 6(b)). Here, the performance gap widens substantially. FlowVLA not only achieves a **55% higher peak success rate** relative to the baseline (0.48 vs. 0.31) but also surpasses the baseline's peak performance in just 1k steps. This substantial improvement in sample efficiency validates our core hypothesis: by requiring the model to explicitly reason about motion via a visual chain-of-thought, FlowVLA benefits from a powerful inductive bias. This simplifies the learning of physical dynamics from raw pixels, leading to a more effective and robust learning process, particularly when data is limited.

3.5. Ablation Studies (Q4)

Finally, we conduct a series of ablation studies to understand the contribution of each key component in our framework. The results, summarized in Table 4, are evaluated on the LIBERO-10 benchmark.

We first remove the entire Visual Chain-of-Thought (CoT) structure, which causes our model to degenerate into the UniVLA baseline. As shown in Table 4, the success rate drops sharply from 73.0% to 64.0%. This

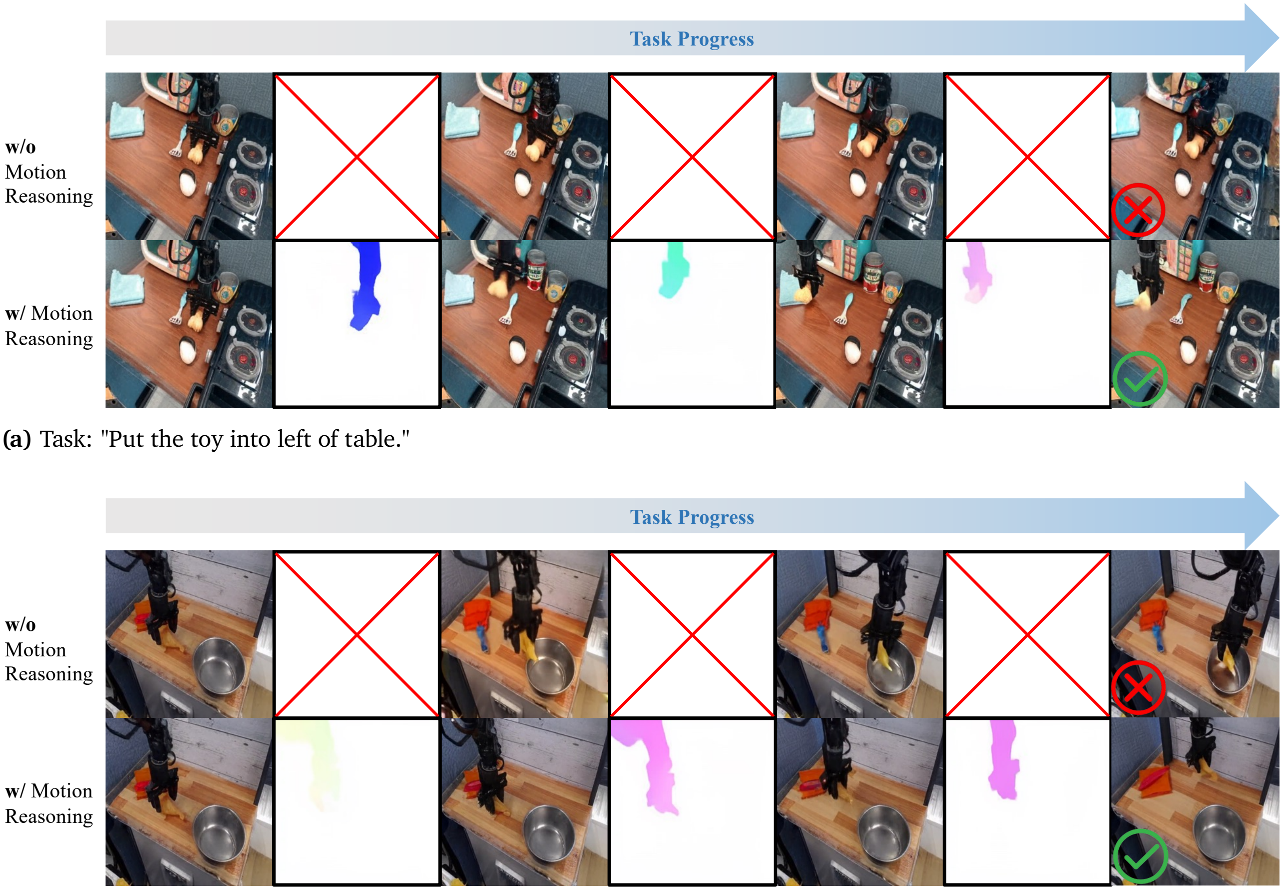

(a) Task: "Put the toy into left of table."

(b) Task: "Move toy diagonally little bit top on the right side."

Figure 5: Analysis of Semantic Alignment on the Bridge V2 Dataset. This figure illustrates the baseline's failure to align predictions with language instructions. While the predicted frames from baseline model (top row) might appear visually plausible at a glance, the resulting motion does not correspond to the specified task (e.g., moving an object in the wrong direction). **FlowVLA** (bottom row) again demonstrates superior performance, correctly interpreting the command and generating a corresponding visual trajectory. This underscores that our Visual CoT not only improves physical realism but also enhances the model's ability to ground language in action.

significant 9-point drop confirms that the explicit, step-by-step reasoning process, where the model first thinks about "how to move" before predicting the outcome, is the primary driver of our model's performance gain.

Next, we investigate the importance of direct supervision for the intermediate reasoning step. In this variant, we retain the interleaved visual-flow sequence structure but remove the optical flow loss during training, meaning the model is not explicitly guided to generate physically correct flows. The performance degrades to 69.5%. This result indicates that while the interleaved architecture provides a useful structural prior, direct supervision is crucial to prevent the model from generating arbitrary or collapsed representations for the intermediate step (f_t). The supervision ensures the "thought" is physically grounded.

Finally, we validate the core design of interleaving information. We restructure the input sequence into the format $v_0, v_1, \ldots, f_0, f_1, \ldots,$ where all visual frames are grouped first, followed by all corresponding flow frames. This configuration leads to a severe performance collapse, with the success rate plummeting to 49.4%.

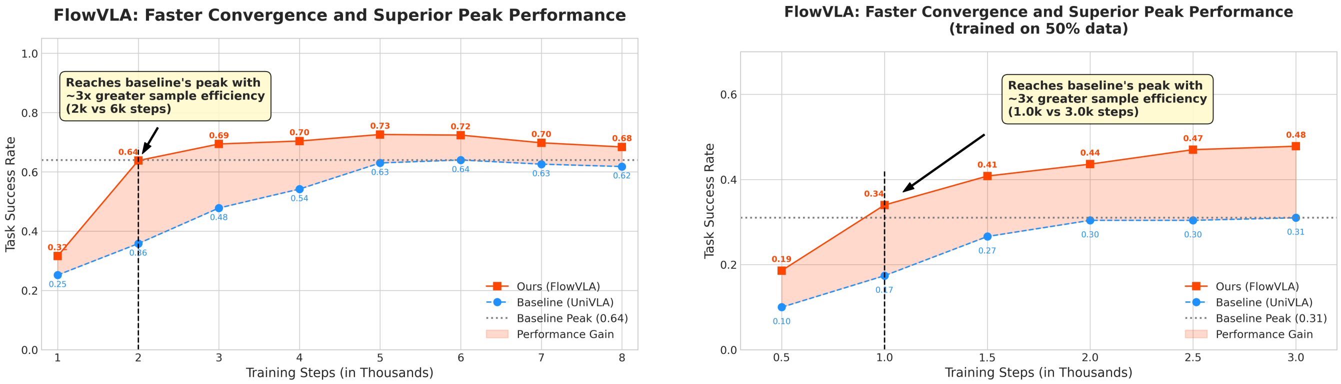

(a) Training on 100% of data

(b) Training on 50% of data

Figure 6: Training Efficiency Comparison in Full and Low-Data Regimes. Success rate versus training steps for FlowVLA and the baseline. Our method converges dramatically faster and reaches a higher peak performance across both the full dataset **(a)** and a data-scarce setting **(b)**. The performance gap widens significantly with limited data, highlighting the superior sample efficiency of our approach.

This is because the model can no longer leverage the predicted motion f_t to inform the generation of the next state v_{t+1} in a causal, forward-looking manner. This result provides strong evidence that the "interleaved, step-by-step causal chain" ($v_t \rightarrow f_t \rightarrow v_{t+1}$) is essential for effective planning and action generation.

Table 4: Ablation studies on the LIBERO-10 benchmark. We evaluate the importance of our key design choices: the Visual CoT structure, the flow supervision loss, and the interleaved sequence format. The full FlowVLA model is shown for comparison.

Configuration	Success Rate (%)
FlowVLA (Ours, Full Model)	**73.0**
Ablations:	
1. w/o CoT (degenerates to baseline)	64.0
2. w/o Flow Loss	69.5
3. Grouped Sequence	49.4

4. Related Work

4.1. Vision-Language-Action (VLA) Models

The dominant paradigm for creating generalist robot agents is the Vision-Language-Action (VLA) model Zitkovich et al. (2023), Kim et al. (2024b), Black et al. (2024), Song et al. (2025b,c). These models extend large, pre-trained Vision-Language Models (VLMs) by fine-tuning them on extensive robotics datasets O'Neill et al. (2024). Architectures like RT-2 Zitkovich et al. (2023), CEED-VLA Song et al. (2025a) and OpenVLA Kim et al. (2024b) treat action generation as a sequence modeling problem, directly mapping visual and textual inputs to discretized action tokens. Other recent works have focused on improving the action representation itself, using techniques like diffusion policies Chi et al. (2023) or flow matching Black et al. (2024). While this end-to-end approach has demonstrated remarkable generalization, it often treats the environment's physical dynamics as a "black box". The policy is learned reactively, without an explicit, underlying model of how the world functions or evolves. FlowVLA diverges from this standard VLA formulation by prioritizing world understanding over immediate action generation. Its pre-training objective is not to learn a policy ($v_t \rightarrow a_t$), but to build a robust world model by learning the physical transition function of the environment ($v_t \rightarrow v_{t+1}$). This "dynamics-first" approach establishes a solid foundation of physical knowledge before it is adapted for downstream control.

4.2. World Models for Robotics

The concept of a world model, which learns a model of its environment to plan or imagine future outcomes Ha and Schmidhuber (2018), is increasingly vital in robotics. Recent works have leveraged this idea for policy learning. For example, some models use video prediction as a form of self-supervised pre-training to improve downstream task performance Wang et al. (2025), Wu et al. (2023). Others, like WorldVLA Cen et al. (2025), propose architectures that jointly learn to predict both the next frame and the next action, creating a tight loop between prediction and control. A common thread in these approaches is the direct prediction of the next frame, modeling the transition as $v_t \rightarrow v_{t+1}$. However, this direct objective forces a single network to simultaneously handle two distinct problems: understanding static scene properties (appearance, texture, lighting) and modeling complex physical dynamics (motion, interaction, causality). This entanglement can result in inefficient learning and physically implausible predictions, such as blurry or distorted futures. In contrast, FlowVLA avoids this entanglement with its Visual Chain of Thought framework. We decompose the prediction into a "frame → flow → frame" reasoning process. By forcing the model to first predict an intermediate optical flow field (f_t), we explicitly decouple the learning of dynamics (*how* things move) from appearance (*what* they look like), resulting in a more causally-grounded world model.

4.3. Embodied Reasoning for Robotics

To move beyond simple reactive policies, a significant line of research has focused on endowing agents with explicit reasoning capabilities. These approaches can be broadly categorized. One category focuses on high-level semantic reasoning, where models generate linguistic or abstract plans. For instance, ECoT Zawalski et al. (2024) and ThinkAct Huang et al. (2025b) leverage Chain-of-Thought prompting to generate textual sub-goals that guide the agent's behavior. A second category focuses on mid-level geometric reasoning, where models produce intermediate spatial representations to guide actions. MolmoAct Lee et al. (2025), for example, generates depth maps and 2D end-effector trajectory traces as part of its "Action Reasoning" pipeline to make planning more concrete. FlowVLA introduces a more fundamental form of reasoning: low-level physical reasoning. Unlike high-level semantic or geometric planning, our Visual CoT operates at the pixel level. By predicting the dense optical flow field, it learns a general, causal model of the world's dynamics, independent of any specific task or action. This provides a foundational understanding of physics that is complementary to, and arguably a prerequisite for, effective high-level control.

5. Conclusion

We proposed the Visual Chain of Thought (Visual CoT) as a new paradigm for world model learning, instantiated in FlowVLA. By decomposing prediction into an explicit *motion–then–appearance* reasoning sequence $v_t \rightarrow f_t \rightarrow v_{t+1}$, our model learns physically grounded representations that align with the demands of downstream action prediction. We introduce a two-stage training paradigm. At the first stage, we pre-train the world model with Visual CoT to build motion-coherent and physically plausible dynamics knowledge from video data. At the second stage, we fine-tune the policy to adapt this knowledge to generate precise robot actions. This design directly addresses the gap between pre-training and fine-tuning in VLA models, leading to improved sample efficiency and robust performance. Experiments on simulation and real-world manipulation benchmarks validate the effectiveness of this motion-first approach, confirming that explicit motion reasoning is a powerful inductive bias for bridging perception and control in generalist robotics.

References

Kevin Black, Noah Brown, Danny Driess, Adnan Esmail, Michael Equi, Chelsea Finn, Niccolo Fusai, Lachy Groom, Karol Hausman, Brian Ichter, Szymon Jakubczak, Tim Jones, Liyiming Ke, Sergey Levine, Adrian Li-Bell, Mohith Mothukuri, Suraj Nair, Karl Pertsch, Lucy Xiaoyang Shi, James Tanner, Quan Vuong, Anna Walling, Haohuan Wang, and Ury Zhilinsky. π_0: A vision-language-action flow model for general robot control, 2024. URL https://arxiv.org/abs/2410.24164.

Jun Cen, Chaohui Yu, Hangjie Yuan, Yuming Jiang, Siteng Huang, Jiayan Guo, Xin Li, Yibing Song, Hao Luo, Fan Wang, et al. Worldvla: Towards autoregressive action world model. *arXiv preprint arXiv:2506.21539*, 2025.

Hila Chefer, Uriel Singer, Amit Zohar, Yuval Kirstain, Adam Polyak, Yaniv Taigman, Lior Wolf, and Shelly Sheynin. VideoJAM: Joint Appearance-Motion Representations for Enhanced Motion Generation in Video Models. *arXiv preprint arXiv:2502.02492*, 2025. URL https://arxiv.org/abs/2502.02492.

Cheng Chi, Zhenjia Xu, Siyuan Feng, Eric Cousineau, Yilun Du, Benjamin Burchfiel, Russ Tedrake, and Shuran Song. Diffusion policy: Visuomotor policy learning via action diffusion. *The International Journal of Robotics Research*, page 02783649241273668, 2023.

Patrick Esser, Robin Rombach, and Bjorn Ommer. Taming transformers for high-resolution image synthesis. In *Proceedings of the IEEE/CVF conference on computer vision and pattern recognition*, pages 12873–12883, 2021.

Zipeng Fu, Tony Z. Zhao, and Chelsea Finn. Mobile aloha: Learning bimanual mobile manipulation with low-cost whole-body teleoperation. In *Conference on Robot Learning (CoRL)*, 2024.

David Ha and Jürgen Schmidhuber. World models. *arXiv preprint arXiv:1803.10122*, 2(3), 2018.

Zhi Hou, Tianyi Zhang, Yuwen Xiong, Haonan Duan, Hengjun Pu, Ronglei Tong, Chengyang Zhao, Xizhou Zhu, Yu Qiao, Jifeng Dai, et al. Dita: Scaling diffusion transformer for generalist vision-language-action policy. *arXiv preprint arXiv:2503.19757*, 2025.

Chi-Pin Huang, Yueh-Hua Wu, Min-Hung Chen, Yu-Chiang Frank Wang, and Fu-En Yang. Thinkact: Vision-language-action reasoning via reinforced visual latent planning. *arXiv preprint arXiv:2507.16815*, 2025a.

Chi-Pin Huang, Yueh-Hua Wu, Min-Hung Chen, Yu-Chiang Frank Wang, and Fu-En Yang. Thinkact: Vision-language-action reasoning via reinforced visual latent planning, 2025b. URL https://arxiv.org/abs/2507.16815.

Heecheol Kim, Yoshiyuki Ohmura, and Yasuo Kuniyoshi. Goal-conditioned dual-action imitation learning for dexterous dual-arm robot manipulation. *IEEE Transactions on Robotics*, 40:2287–2305, 2024a. doi: 10.1109/TRO.2024.3372778.

Moo Jin Kim, Karl Pertsch, Siddharth Karamcheti, Ted Xiao, Ashwin Balakrishna, Suraj Nair, Rafael Rafailov, Ethan Foster, Grace Lam, Pannag Sanketi, et al. Openvla: An open-source vision-language-action model. *arXiv preprint arXiv:2406.09246*, 2024b.

Moo Jin Kim, Chelsea Finn, and Percy Liang. Fine-tuning vision-language-action models: Optimizing speed and success, 2025. URL https://arxiv.org/abs/2502.19645.

Jason Lee, Jiafei Duan, Haoquan Fang, Yuquan Deng, Shuo Liu, Boyang Li, Bohan Fang, Jieyu Zhang, Yi Ru Wang, Sangho Lee, Winson Han, Wilbert Pumacay, Angelica Wu, Rose Hendrix, Karen Farley, Eli VanderBilt, Ali Farhadi, Dieter Fox, and Ranjay Krishna. Molmoact: Action reasoning models that can reason in space, 2025. URL https://arxiv.org/abs/2508.07917.

Xuanlin Li, Kyle Hsu, Jiayuan Gu, Karl Pertsch, Oier Mees, Homer Rich Walke, Chuyuan Fu, Ishikaa Lunawat, Isabel Sieh, Sean Kirmani, et al. Evaluating real-world robot manipulation policies in simulation. *arXiv preprint arXiv:2405.05941*, 2024.

Bo Liu, Yifeng Zhu, Chongkai Gao, Yihao Feng, Qiang Liu, Yuke Zhu, and Peter Stone. Libero: Benchmarking knowledge transfer for lifelong robot learning. *Advances in Neural Information Processing Systems*, 36: 44776–44791, 2023.

Huaping Liu, Xinghang Li, Peiyan Li, Minghuan Liu, Dong Wang, Jirong Liu, Bingyi Kang, Xiao Ma, Tao Kong, and Hanbo Zhang. Towards generalist robot policies: What matters in building vision-language-action models. 2025.

Ruibo Ming, Zhewei Huang, Zhuoxuan Ju, Jianming Hu, Lihui Peng, and Shuchang Zhou. A survey on video prediction: From deterministic to generative approaches. *CoRR*, 2024.

Abby O'Neill, Abdul Rehman, Abhiram Maddukuri, Abhishek Gupta, Abhishek Padalkar, Abraham Lee, Acorn Pooley, Agrim Gupta, Ajay Mandlekar, Ajinkya Jain, et al. Open x-embodiment: Robotic learning datasets and rt-x models: Open x-embodiment collaboration 0. In *2024 IEEE International Conference on Robotics and Automation (ICRA)*, pages 6892–6903. IEEE, 2024.

Karl Pertsch, Kyle Stachowicz, Brian Ichter, Danny Driess, Suraj Nair, Quan Vuong, Oier Mees, Chelsea Finn, and Sergey Levine. Fast: Efficient action tokenization for vision-language-action models. *arXiv preprint arXiv:2501.09747*, 2025.

Delin Qu, Haoming Song, Qizhi Chen, Yuanqi Yao, Xinyi Ye, Yan Ding, Zhigang Wang, JiaYuan Gu, Bin Zhao, Dong Wang, et al. Spatialvla: Exploring spatial representations for visual-language-action model. *arXiv preprint arXiv:2501.15830*, 2025.

Wenxuan Song, Jiayi Chen, Pengxiang Ding, Yuxin Huang, Han Zhao, Donglin Wang, and Haoang Li. Ceed-vla: Consistency vision-language-action model with early-exit decoding, 2025a. URL https://arxiv.org/abs/2506.13725.

Wenxuan Song, Jiayi Chen, Pengxiang Ding, Han Zhao, Wei Zhao, Zhide Zhong, Zongyuan Ge, Jun Ma, and Haoang Li. Accelerating vision-language-action model integrated with action chunking via parallel decoding, 2025b. URL https://arxiv.org/abs/2503.02310.

Wenxuan Song, Ziyang Zhou, Han Zhao, Jiayi Chen, Pengxiang Ding, Haodong Yan, Yuxin Huang, Feilong Tang, Donglin Wang, and Haoang Li. Reconvla: Reconstructive vision-language-action model as effective robot perceiver. *arXiv preprint arXiv:2508.10333*, 2025c.

Octo Model Team, Dibya Ghosh, Homer Walke, Karl Pertsch, Kevin Black, Oier Mees, Sudeep Dasari, Joey Hejna, Tobias Kreiman, Charles Xu, et al. Octo: An open-source generalist robot policy. *arXiv preprint arXiv:2405.12213*, 2024.

Zachary Teed and Jia Deng. Raft: Recurrent all-pairs field transforms for optical flow. In *European conference on computer vision*, pages 402–419. Springer, 2020.

Xinlong Wang, Xiaosong Zhang, Zhengxiong Luo, Quan Sun, Yufeng Cui, Jinsheng Wang, Fan Zhang, Yueze Wang, Zhen Li, Qiying Yu, Yingli Zhao, Yulong Ao, Xuebin Min, Tao Li, Boya Wu, Bo Zhao, Bowen Zhang, Liangdong Wang, Guang Liu, Zheqi He, Xi Yang, Jingjing Liu, Yonghua Lin, Tiejun Huang, and Zhongyuan Wang. Emu3: Next-token prediction is all you need, 2024. URL https://arxiv.org/abs/2409.18869.

Yuqi Wang, Xinghang Li, Wenxuan Wang, Junbo Zhang, Yingyan Li, Yuntao Chen, Xinlong Wang, and Zhaoxiang Zhang. Unified vision-language-action model, 2025. URL https://arxiv.org/abs/2506.19850.

Jason Wei, Xuezhi Wang, Dale Schuurmans, Maarten Bosma, Fei Xia, Ed Chi, Quoc V Le, Denny Zhou, et al. Chain-of-thought prompting elicits reasoning in large language models. *Advances in neural information processing systems*, 35:24824–24837, 2022.

Hongtao Wu, Ya Jing, Chilam Cheang, Guangzeng Chen, Jiafeng Xu, Xinghang Li, Minghuan Liu, Hang Li, and Tao Kong. Unleashing large-scale video generative pre-training for visual robot manipulation. *arXiv preprint arXiv:2312.13139*, 2023.

Zisong Xu, Rafael Papallas, Jaina Modisett, Markus Billeter, and Mehmet R. Dogar. Tracking and control of multiple objects during nonprehensile manipulation in clutter. *IEEE Transactions on Robotics*, 41: 3929–3947, 2025. doi: 10.1109/TRO.2025.3577437.

Wentao Yuan, Jiafei Duan, Valts Blukis, Wilbert Pumacay, Ranjay Krishna, Adithyavairavan Murali, Arsalan Mousavian, and Dieter Fox. Robopoint: A vision-language model for spatial affordance prediction for robotics. *arXiv preprint arXiv:2406.10721*, 2024.

Yifu Yuan, Haiqin Cui, Yibin Chen, Zibin Dong, Fei Ni, Longxin Kou, Jinyi Liu, Pengyi Li, Yan Zheng, and Jianye Hao. From seeing to doing: Bridging reasoning and decision for robotic manipulation. *arXiv preprint arXiv:2505.08548*, 2025a.

Yifu Yuan, Haiqin Cui, Yaoting Huang, Yibin Chen, Fei Ni, Zibin Dong, Pengyi Li, Yan Zheng, and Jianye Hao. Embodied-r1: Reinforced embodied reasoning for general robotic manipulation, 2025b. URL https://arxiv.org/abs/2508.13998.

Michał Zawalski, William Chen, Karl Pertsch, Oier Mees, Chelsea Finn, and Sergey Levine. Robotic control via embodied chain-of-thought reasoning. *arXiv preprint arXiv:2407.08693*, 2024.

Jia Zeng, Qingwen Bu, Bangjun Wang, Wenke Xia, Li Chen, Hao Dong, Haoming Song, Dong Wang, Di Hu, Ping Luo, et al. Learning manipulation by predicting interaction. *arXiv preprint arXiv:2406.00439*, 2024.

Qingqing Zhao, Yao Lu, Moo Jin Kim, Zipeng Fu, Zhuoyang Zhang, Yecheng Wu, Zhaoshuo Li, Qianli Ma, Song Han, Chelsea Finn, et al. Cot-vla: Visual chain-of-thought reasoning for vision-language-action models. In *Proceedings of the Computer Vision and Pattern Recognition Conference*, pages 1702–1713, 2025.

Tony Z Zhao, Vikash Kumar, Sergey Levine, and Chelsea Finn. Learning fine-grained bimanual manipulation with low-cost hardware. *arXiv preprint arXiv:2304.13705*, 2023.

Ruijie Zheng, Yongyuan Liang, Shuaiyi Huang, Jianfeng Gao, Hal Daumé III, Andrey Kolobov, Furong Huang, and Jianwei Yang. Tracevla: Visual trace prompting enhances spatial-temporal awareness for generalist robotic policies. *arXiv preprint arXiv:2412.10345*, 2024.

Jianshu Zhou, Junda Huang, Qi Dou, Pieter Abbeel, and Yunhui Liu. A dexterous and compliant (dexco) hand based on soft hydraulic actuation for human-inspired fine in-hand manipulation. *IEEE Transactions on Robotics*, 41:666–686, 2025. doi: 10.1109/TRO.2024.3508932.

Brianna Zitkovich, Tianhe Yu, Sichun Xu, Peng Xu, Ted Xiao, Fei Xia, Jialin Wu, Paul Wohlhart, Stefan Welker, Ayzaan Wahid, et al. Rt-2: Vision-language-action models transfer web knowledge to robotic control. In *Conference on Robot Learning*, pages 2165–2183. PMLR, 2023.